



Strong tremor near Parkfield, CA, excited by the 2002 Denali Fault earthquake

Zhigang Peng,¹ John E. Vidale,² Kenneth C. Creager,² Justin L. Rubinstein³
Joan Gomberg,⁴ and Paul Bodin²

Received 21 September 2008; revised 22 October 2008; accepted 27 October 2008; published 5 December 2008.

[1] We show clear evidence of non-volcanic tremor triggered by 2002 Mw7.8 Denali Fault earthquake near Parkfield. Triggered tremor is identified as bursts of high-frequency ($\sim 2\text{--}8$ Hz), non-impulsive seismic energy whose envelope is coherent among many stations and has the same periodicity as the passing surface waves. The tremor originates from at least three hypocenters near the San Andreas fault with differing frictional regimes, two in the creeping section and the other where the San Andreas is transitional between creeping and locked. All the sources originate below the seismogenic zone, suggesting that transitional frictional properties are necessary conditions for tremor generation. Tremor is excited by the Love waves when the San Andreas is sheared in a right-lateral sense, encouraging slip, and is absent when the San Andreas is sheared in a left-lateral sense, consistent with a simple frictional response to the driving stress. **Citation:** Peng, Z., J. E. Vidale, K. C. Creager, J. L. Rubinstein, J. Gomberg, and P. Bodin (2008), Strong tremor near Parkfield, CA, excited by the 2002 Denali Fault earthquake, *Geophys. Res. Lett.*, 35, L23305, doi:10.1029/2008GL036080.

1. Introduction

[2] Non-volcanic tremor (NVT) is a seismic signal with long durations and no clear body wave arrivals, and with spectra depleted in high-frequency energy compared with regular earthquakes of similar amplitude. NVT was originally identified in a subduction zone southwest of Japan [Obara, 2002]. Subsequent studies have found NVT in many circum-Pacific subduction zones [e.g., Rogers and Dragert, 2003; Schwartz and Rokosky, 2007]. The tremor is often found during episodic slow-slip events, and together they are called as Episodic Tremor and Slip (ETS) [Rogers and Dragert, 2003].

[3] In addition to occurring in protracted ETS event, NVT can also be triggered by the surface waves of teleseismic events both in subduction and other tectonic environments [Miyazawa and Mori, 2005, 2006; Miyazawa and Brodsky, 2008; Rubinstein et al., 2007; Gomberg et al., 2008; Peng and Chao, 2008]. However, the underlying

process for triggered tremor remains unclear. Some studies propose that fluid flow due to changes in dilatational stresses associated with the Rayleigh waves trigger NVT [Miyazawa and Mori, 2005, 2006], while others suggest that perturbation of Coulomb failure stresses on the fault interface directly and instantaneously trigger NVT [Rubinstein et al., 2007; Peng and Chao, 2008].

[4] In this study, we analyze the tremor triggered by the 11/03/2002 Mw7.8 Denali Fault earthquake [Gomberg et al., 2008], and recorded by many stations near the Parkfield section of the SAF (Figure 1). We focused around Parkfield because it is one of the few places outside the subduction zone environment where ambient tremor has been identified [Nadeau and Dolenc, 2005], and there is an unprecedented density of instrumentation there, which promise to reveal details of tremor sources with unprecedented fidelity.

2. Observations of the Triggered Tremor

[5] We identify triggered NVT as bursts of $\sim 2\text{--}8$ Hz, non-impulsive seismic energy whose envelope is coherent among many stations and has the same periodicity as the passing surface waves. Figure 2 shows a comparison of the broadband recordings of the Denali Fault earthquake and the band-pass-filtered seismograms from station PKD. This station contains a Streckeisen STS-2 Seismometer and is part of the Berkeley Digital Seismic Network. The energy associated with the teleseismic *P* waves of the Denali Fault earthquake is visible up to 3 Hz. In addition, we find bursts of higher-frequency energy during the large-amplitude surface waves. No impulsive body wave arrivals can be identified within most of the bursts. However, the high-frequency bursts are coherent for stations across an aperture of several tens of kilometers, and have hyperbola-type moveout along the SAF fault strike (Figure 3). This pattern indicates that they are not generated by instrumental noise [Hellweg et al., 2008] or dynamic triggering in the near surface [Fischer et al., 2008], nor are they waves generated outside the network, but are produced by locally triggered tremor [Gomberg et al., 2008]. The similarity in spectral shapes between the ambient and triggered tremor supports this conclusion (Figure S1).¹ Both NVT types are deficient in high frequencies relative to regular earthquakes. The triggered tremor is larger in amplitude by a factor of ten than typical ambient tremor, consistent with triggered tremor on Vancouver Island [Rubinstein et al., 2007].

[6] We locate the triggered NVT with a grid search over possible locations. This is the same method used by

¹School of Earth and Atmospheric Sciences, Georgia Institute of Technology, Atlanta, Georgia, USA.

²Department of Earth and Space Sciences, University of Washington, Seattle, Washington, USA.

³U.S. Geological Survey, Menlo Park, California, USA.

⁴U.S. Geological Survey, Seattle, Washington, USA.

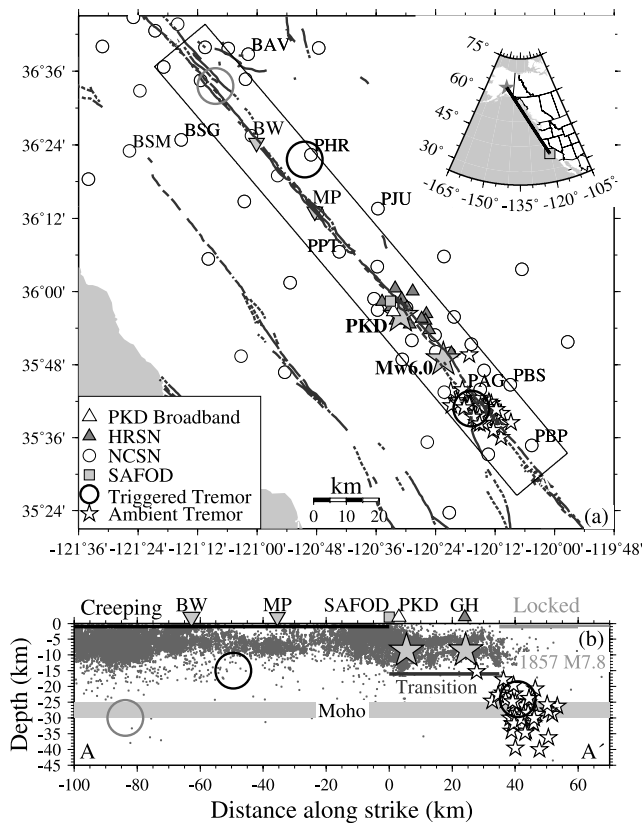


Figure 1. (a) A map of the study area around the Parkfield section of the San Andreas fault. The dark lines denote surface traces of active faults. Seismic stations of the HRSN and NCSN are denoted with gray triangles and white circles. The broadband station PKD is shown as a white triangle. The hypocenters of the 1966 and 2004 M6 Parkfield earthquakes are marked with large gray stars. The ambient tremor previously identified by *Nadeau and Dolenc* [2005] is denoted as the white star. The two strong tremor source regions are denoted with the solid circles, and a possible weak tremor source region further north is marked as the gray circle. The inset shows the epicenter of the 2002 Mw7.8 Denali Fault earthquake (star), the SAFOD (square), and the great circle ray path. (b) Cross-section of seismicity and location of tremor sources along AA' in Figure 1a. The gray dots denote earthquakes since 1984 listed in the NCSN catalog. The Moho depth of 25–30 km in this region [McBride and Brown, 1986] is marked as a gray band. The dark, gray, and light gray lines mark the approximate creeping, transition, and locked segments on the SAF. BW: Bitterwater; MP: Monarch Peak; GH: Gold Hill.

Rubinstein et al. [2007], and is similar to that used by *Obara* [2002]. In detail, we calculate cross-correlograms of envelopes from pairs of 2–8 Hz band-pass-filtered vertical-component seismograms. As has been the case for tremor in previous studies [Obara, 2002], we find the NVT has a moveout with distance matching the *S*-wave velocity (Figure S2). For each trial source location, we calculate the *S*-wave travel time difference for each station pair and determine the value of the correlation at that predicted lag time. We find the location that maximizes the sum of

weighted correlations using an L-1 norm [Wech and Creager, 2007]. The *S*-wave velocity model is computed from a 1D *P*-wave velocity V_p model used by *Waldhauser et al.* [2004] by assuming the V_p/V_s ratio of 1.732. We have also tried a “local” V_p/V_s ratio of 1.78 above 8 km, and 1.732 below 8 km (H. Zhang, personal communication, 2007). This result in minor decrease of the depth, but virtually no effect on the epicenter.

[7] We identify two strong tremor source regions near Parkfield and a possible weak source region further north (Figure 1). The tremor moveout south of Parkfield is well explained by a single tremor source near Cholame at $(-120.28^\circ \pm 5 \text{ km}, 35.68^\circ \pm 5 \text{ km})$, where the SAF slip behavior is transitional between creeping and locked, and where ambient tremor had already been found [Nadeau and Dolenc, 2005]. The tremor recorded by stations north of Parkfield is more complicated, suggesting the possibility of multiple sources in that region. A strong tremor source is located at $(-120.84^\circ \pm 5 \text{ km}, 36.36^\circ \pm 10 \text{ km})$ in the creeping section of the SAF between Monarch Peak and Bitterwater (Figure 1). We also find evidence of a weak tremor source occurring around stations BAV, BSG, and BSM north of Bitterwater. The tremor peaks shown in the

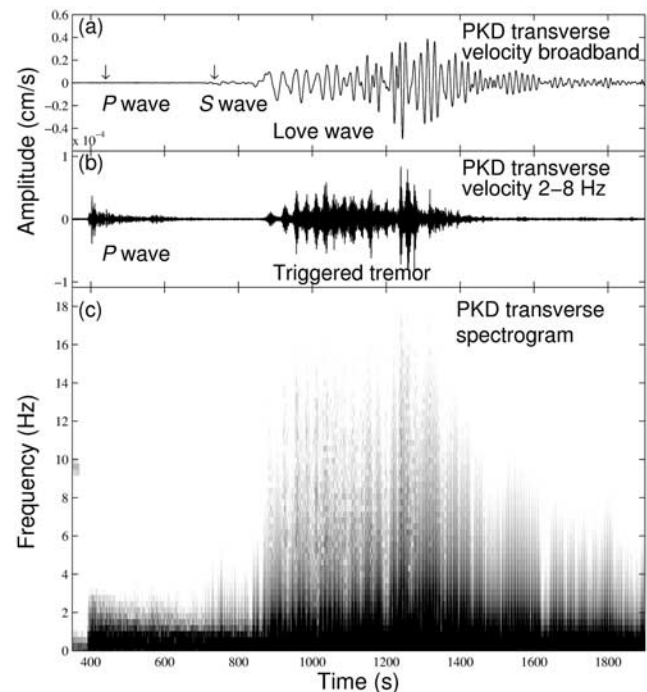


Figure 2. Example of triggered tremor during the surface waves of the 2002 Mw7.8 Denali Fault earthquake. (a) Broadband transverse-component seismogram recorded at station PKD. The two arrows mark the approximate arrival times of the *P* and *S* waves. (b) 2–8 Hz bandpass-filtered transverse-component seismogram showing the high-frequency *P* waves and the triggered tremors during the passage of the surface waves. (c) The spectrogram of the transverse-component seismogram from station PKD. The triggered tremors are shown as narrow vertical bands rich in high-frequency energy. The weak signal around 10 Hz before the arrival of the *P* waves does not appear on other stations, thus we believe it is not associated with tremor.

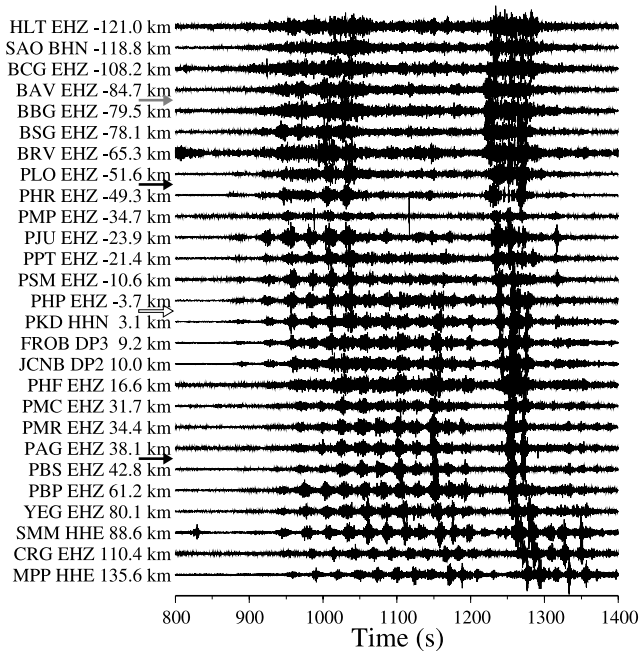


Figure 3. A record section of the 2–8 Hz band-pass-filtered seismograms showing moveout of the tremor from two strong source regions (marked by the dark arrows), and a possible weak source region (the gray arrow) further north. The seismograms are plotted according to the along-strike distance on the SAF, with NW on the top and SE on the bottom. The open arrow marks the location of the SAFOD. We only show seismograms recorded on-scale at stations close (within 20 km) to the SAF strike and with relatively clean tremor signals. The station and channel names, and the along-strike distance relative to the SAFOD are marked on the left of the corresponding traces.

envelope functions for these stations arrive several seconds earlier than those for stations (e.g., PHR, PJU, PPT) further south along the SAF (Figure 3). However, the absolute amplitudes of tremor bursts (Figure S3) for these stations (BAV, BSG, and BSM) are 2–3 times smaller than those stations in the south (e.g., PHR, PJU, and PPT). Hence, we suggest that a weak tremor was activated earlier and recorded only by stations BAV, BSG, and BSM, while the strong tremor occurred slightly later and was recorded by many stations north of Parkfield. Because of this, we will focus in the following sections on the two strong tremor sources south of Parkfield near Cholame, and north of Parkfield between Monarch Peak and Bitterwater.

[8] A few details warrant additional comment. First, it is worth noting that we did not constrain the number of source regions in our location procedure. Instead, we find from the misfit maps (Figure S4) that two strong source regions are sufficient to explain the moveout of tremor envelopes observed around Parkfield (Figure 3). The only exception is the aforementioned tremor observed near stations BAV, BSG, and BSM, which could be produced by an additional weak tremor source. As was found in previous studies, the tremor source depths are less well constrained. The best-fitting depths for the southern and northern tremor sources are 24 ± 10 km and 15 ± 10 km, respectively. Finally, our location procedure does not resolve differences between the

epicenters of individual tremor pulses, although from difficulty in matching the entire envelope at all the stations, we suspect the source regions fill some volume. Attempts to analyze individual pulses separately have not yielded well-resolved location differences.

3. Correlations Between Tremor and Surface Waves

[9] Next, we align the tremor with the surface waves of the Denali Fault earthquake in Figure 4. This involves two corrections. We must shift (1) the surface waves to account for the time between the surface waves passing the reference broadband station PKD and the source region, and (2) the tremor envelopes to account for the shear wave travel time to the station from the source region.

[10] For the first correction, we shift the surface waves by an average phase velocity of 4.1 km/s, measured from seismograms recorded by nearby broadband stations (Figure S5). This has uncertainty of ± 1 s due to dispersion of the surface waves, but this is similar to the potential errors from the depth uncertainty. As the phase of the surface wave varies little with depth, we do not make a depth phase correction.

[11] For the second correction, the time shift for the tremor envelope is calculated from the 1D velocity model and trial locations. We normalize the time-shifted tremor envelopes observed at the 7–8 nearest stations, and stack them to produce the tremor source functions for each source region (Figure S2). We observe good agreement of the

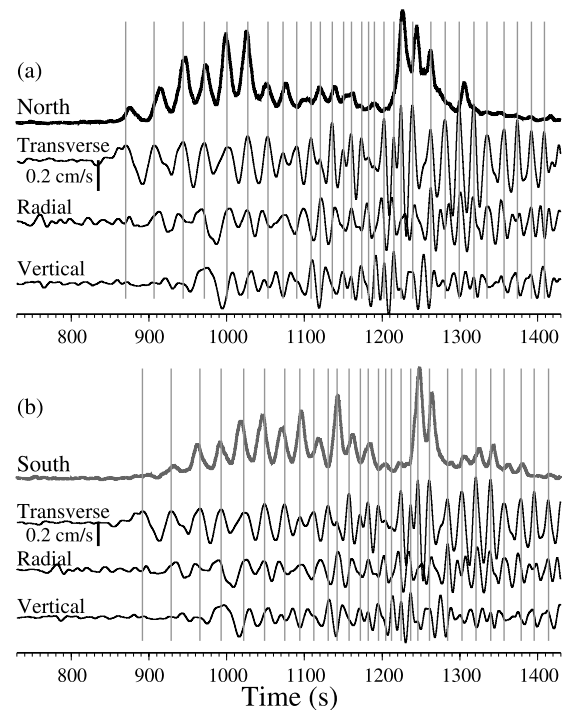


Figure 4. Tremor envelope functions observed north (a) and south (b) of Parkfield compared with the surface wave velocities after shifting them back to the tremor source regions. The vertical lines mark the peaks when the transverse component is to the southwest (i.e., promoting the right-lateral slip on the SAF).

phasing of the NVT with the first eight Love wave cycles for the southern region, and a less precise match for the first eight tremor peaks for the northern region (Figure 4).

[12] The fundamental-mode Love surface waves exert strong right- and left-lateral shear stresses resolved on the SAF. The near-coincidence of the strike of the SAF fault and the great-circle path from Alaska result in the along-strike stress being proportional to the Love wave velocity. This is because the along-strike stress on a vertical strike-slip fault aligned with the propagation direction arises from radial-direction gradients in the Love wave particle displacement [e.g., Hill, 2008], which for a single frequency is equal to the ratio of the particle and Love wave phase velocities and 180° opposite in phase. In our case of waves traveling southeast, it is the velocity to the southwest that encourage NVT by boosting right-lateral stress, and velocity to the northeast that discourage it, and this is the observed correlation. In comparison, the normal stress is mainly associated with Rayleigh waves, which is proportional to a linear combination of the vertical displacement and radial velocity. Since we do not observe clear correlation between the tremor envelope with the Rayleigh wave velocity (Figure 4) and displacement (Figure S6), we argue that the tremor is mainly caused by shear stresses induced by the passage of the Love waves.

[13] We estimate the amplitude of the shear stresses associated with the Love waves encouraging slip on the plate interface to be on the order of 10 to 20 kPa. This extrapolation from the Love wave velocity amplitude at the surface to the stress amplitude at the tremor source depth requires knowledge of the decrease in Love wave amplitude and the increase in rigidity with depth, which we compute using a locked-mode surface wave code [Gomberg and Masters, 1988] and a 1D velocity model around the Parkfield region.

4. Discussions

[14] Figure 1b shows a comparison of seismicity and tremor locations around the Parkfield section of the SAF, which straddles the transition between the creeping segment of the fault to the northwest and the locked segment to the southeast. These differing ambient slip behaviors likely reflect different frictional properties within the seismogenic zone, above ~ 10 – 15 km as inferred from the maximum depth of microseismicity. Apparently these differences have little impact on tremor generation. Our best fitting depth for both tremor sources is ~ 15 – 24 km, below the seismogenic zone and close to the depth range of 20–40 km for the ambient tremor [Nadeau and Dolenc, 2005]. This suggests tremor generation requires transitional frictional properties as well as other conditions found at depths below where earthquake typically occur. Possible conditions include temperature, pressure, rock type, frictional properties, and pore-fluid pressures. At the current stage, it is still not clear what are the necessary conditions for tremor generation.

[15] This study presents several complications not seen in case of Vancouver Island [Rubinstein et al., 2007]. The first complication is that tremor burst amplitudes are not proportional to the corresponding Love wave amplitudes, rather the tremor peaks grow over time while the peak stresses change much less. This is true for both the northern and

southern source regions, with the southern source particularly anemic at the onset. The second complication is that the NVT does not persist as long as the surface waves. The northern source dies out after just 6 cycles, the south lasts longer, but both fade away before the strong surface waves end. A third feature is a strong stage of tremor between 1200 and 1300 s. Based on the misfit map (Figure S4), it appears that the later arriving pulses of energy originated from similar locations to the earlier triggered tremor. However, it is not clear what causes the break in the tremor activity as the surface waves were still ongoing during that time period.

[16] So far, triggered and ambient tremor for both subduction and strike slip regimes have much in common, and do not yet require any differences in mechanism. This mechanism, though, remains unknown. The relatively low triggering threshold (on the order of a few tens of kPa or less), together with recent observations of tidal modulation [Shelly et al., 2007; Rubinstein et al., 2008; Nakata et al., 2008], suggests that NVT is very sensitive to external stress perturbation. We note that NVT is not triggered everywhere by large teleseismic events, indicating that other conditions are needed for their occurrence. Triggered NVT observations in diverse tectonic environments will not only help to better quantify the triggering mechanisms and necessary conditions, but also improve our understanding of fundamental faulting processes.

[17] **Acknowledgments.** The data used in this study come from the High Resolution Seismic Network operated by Berkeley Seismological Laboratory, University of California, Berkeley, the Northern California Seismic Network (NCSN) operated by the U.S. Geological Survey, Menlo Park, and are distributed by the northern California earthquake data center. We thank David Oppenheimer and Doug Neuhauser for extracting the high-sampling rate NCSN data used in this study, and Bob Nadeau for sharing his ambient tremor catalog with us. We also thank the editor and two anonymous reviewers for the constructive comments. The study was supported by the National Science Foundation (grant EAR-0809834: ZP; grant EAR-0809993: JEV).

References

- Fischer, A., Z. Peng, and C. G. Sammis (2008), Dynamic triggering of high-frequency bursts by strong motions during the 2004 Parkfield earthquake sequence, *Geophys. Res. Lett.*, *35*, L12305, doi:10.1029/2008GL033905.
- Gomberg, J., and T. G. Masters (1988), Waveform modeling using locked-mode synthetic and differential seismograms: Application to determination of the structure of Mexico, *Geophys. J. Int.*, *94*, 193–218.
- Gomberg, J., J. L. Rubinstein, Z. Peng, K. C. Creager, and J. E. Vidale (2008), Widespread triggering of non-volcanic tremor in California, *Science*, *319*, 173, doi:10.1126/science.1149164.
- Hellweg, M., R. A. Uhrhammer, S. Ford, and J. Friday (2008), Nonvolcanic tremor in Denali surface waves at broadband stations in northern California: Instrumental causes?, *Seismol. Res. Lett.*, *79*, 327.
- Hill, D. P. (2008), Dynamic stresses, coulomb failure, and remote triggering, *Bull. Seismol. Soc. Am.*, *98*, 66–92, doi:10.1785/0120070049.
- McBride, J., and L. D. Brown (1986), Reanalysis of the COCORP deep seismic reflection profile across the San Andreas fault, Parkfield, CA, *Bull. Seismol. Soc. Am.*, *76*, 1668–1686.
- Miyazawa, M., and E. E. Brodsky (2008), Deep low-frequency tremor that correlates with the passing surface waves, *J. Geophys. Res.*, *113*, B01307, doi:10.1029/2006JB004890.
- Miyazawa, M., and J. Mori (2005), Detection of triggered deep low-frequency events from the 2003 Tokachi-oki earthquake, *Geophys. Res. Lett.*, *32*, L10307, doi:10.1029/2005GL022539.
- Miyazawa, M., and J. Mori (2006), Evidence suggesting fluid flow beneath Japan due to periodic seismic triggering from the 2004 Sumatra-Andaman earthquake, *Geophys. Res. Lett.*, *33*, L05303, doi:10.1029/2005GL020587.
- Nadeau, R. M., and D. Dolenc (2005), Nonvolcanic tremors deep beneath the San Andreas Fault, *Science*, *307*, 389–389.

- Nakata, R., N. Suda, and H. Tsuruoka (2008), Non-volcanic tremor resulting from the combined effects of Earth tides and slow slip events, *Nature Geosci.*, *1*, 676–678, doi:10.1038/ngeo288.
- Obara, K. (2002), Nonvolcanic deep tremor associated with subduction in southwest Japan, *Science*, *296*, 1679–1681.
- Peng, Z., and K. Chao (2008), Non-volcanic tremor beneath the Central Range in Taiwan triggered by the 2001 *Mw*7.8 Kunlun earthquake, *Geophys. J. Int.*, 825–829, doi:10.1111/j.1365-246X.2008.03886.x.
- Rogers, G., and H. Dragert (2003), Episodic tremor and slip on the Cascadia subduction zone: The chatter of silent slip, *Science*, *300*, 1942–1943.
- Rubinstein, J. L., J. E. Vidale, J. Gomberg, P. Bodin, K. C. Creager, and S. D. Malone (2007), Non-volcanic tremor driven by large transient shear stresses, *Nature*, *448*, 579–582.
- Rubinstein, J. E., M. La Rocca, J. E. Vidale, K. C. Creager, and A. G. Wech (2008), Tidal modulation of nonvolcanic tremor, *Science*, *319*, 186–189.
- Schwartz, S. Y., and J. M. Rokosky (2007), Slow slip events and seismic tremor at circum-Pacific subduction zones, *Rev. Geophys.*, *45*, RG3004, doi:10.1029/2006RG000208.
- Shelly, D. R., G. C. Beroza, and S. Ide (2007), Complex evolution of transient slip derived from precise tremor locations in western Shikoku, Japan, *Geochem. Geophys. Geosyst.*, *8*, Q10014, doi:10.1029/2007GC001640.
- Waldhauser, F., W. L. Ellsworth, D. P. Schaff, and A. Cole (2004), Streaks, multiplets, and holes: High-resolution spatio-temporal behavior of Parkfield seismicity, *Geophys. Res. Lett.*, *31*, L18608, doi:10.1029/2004GL020649.
- Wech, A. G., and K. C. Creager (2007), Cascadia tremor polarization evidence for plate interface slip, *Geophys. Res. Lett.*, *34*, L22306, doi:10.1029/2007GL031167.

P. Bodin, K. C. Creager, and J. E. Vidale, Department of Earth and Space Sciences, University of Washington, Box 351310, Seattle, WA 98195, USA.

J. Gomberg, U.S. Geological Survey, Department of Earth and Space Sciences, University of Washington, Box 351310, Seattle, WA 98195, USA.

Z. Peng, School of Earth and Atmospheric Sciences, Georgia Institute of Technology, Atlanta, GA 30332, USA. (zpeng@gatech.edu)

J. L. Rubinstein, U.S. Geological Survey, 345 Middlefield Road/MS-977, Menlo Park, CA 94025, USA.